



Ion, R., Hudson, C., Johnson, J., Yuan, W., Heesom, K., & López Bernal, A. (2018). Smoking alters hydroxyprostaglandin dehydrogenase expression in fetal membranes. *Reproductive Toxicology*, 82, 18-24. <https://doi.org/10.1016/j.reprotox.2018.09.004>

Peer reviewed version

Link to published version (if available):
[10.1016/j.reprotox.2018.09.004](https://doi.org/10.1016/j.reprotox.2018.09.004)

[Link to publication record in Explore Bristol Research](#)
PDF-document

This is the author accepted manuscript (AAM). The final published version (version of record) is available online via Elsevier at <https://doi.org/10.1016/j.reprotox.2018.09.004>. Please refer to any applicable terms of use of the publisher.

University of Bristol - Explore Bristol Research

General rights

This document is made available in accordance with publisher policies. Please cite only the published version using the reference above. Full terms of use are available: <http://www.bristol.ac.uk/red/research-policy/pure/user-guides/ebr-terms/>

Smoking alters hydroxyprostaglandin dehydrogenase expression in fetal membranes

Rachel Ion^{a,b}, Claire Hudson^{b,c}, Jason Johnson^c, Wei Yuan^d, Kate Heesom^e, Andrés López Bernal^{a,b}

^aDepartment of Obstetrics and Gynecology, Level D, St Michael's Hospital, Southwell Street, Bristol BS2 8EG UK.

^bUniversity of Bristol, Dorothy Hodgkin Building, Whitson Street, Bristol, BS1 3NY, UK

^cUniversity of Bristol School of Clinical Sciences, Level 7, Bristol Royal Infirmary, Upper Maudlin Street, Bristol, BS2 8HW, UK

^dDepartment of Clinical Studies, The Institute of Cancer Research, 123 Old Brompton Road, London SW7 3RP. UK

^eUniversity of Bristol Proteomics Facility, Biomedical Sciences Building, University Walk, Clifton, Bristol. BS8 1TD. UK.

Corresponding author: ionrc@hotmail.com

claire.hudson@bristol.ac.uk

jason.l.johnson@bristol.ac.uk

wei.yuan@icr.ac.uk

k.heesom@bristol.ac.uk

a.lopezbernal@bristol.ac.uk

Abstract

Introduction The way in which tobacco smoking increases the risk of preterm labor remains uncertain. Altered prostaglandin metabolism is one potential mechanism.

Methods Proteins in fetal membrane samples (amniochoriodecidua) from 20 women were relatively quantified using Tandem Mass Tagging nano-liquid chromatography mass spectrometry.

Results Prostaglandin synthases and two enzymes involved in prostaglandin degradation, hydroxyprostaglandin dehydrogenase (HPGD) and CBR1, were detected by the mass spectrometer. The expression of HPGD was significantly lower in smokers relative to non-smokers (0.43 fold, $p=0.016$). There was no effect of labor, inflammatory status or gestational age on the HPGD levels.

Discussion We describe for the first time an association between maternal smoking and HPGD expression. We propose that reduced expression of HPGD is one mechanism through which smoking may contribute to preterm labor. Lower levels of this enzyme, key to metabolising prostaglandins, may result in higher levels of prostaglandins and therefore precipitate labor prematurely.

Keywords: uterine proteome; fetal membranes; pregnancy; birth; labor; smoking; prematurity

Abbreviations: PGF2 α (prostaglandin F2 α), PGE2 (prostaglandin E2), PGD2 (prostaglandin D2), HPGD (15-hydroxyprostaglandin dehydrogenase).

Introduction

Smoking is known to increase the risk of both spontaneous and iatrogenic preterm birth, but the association with spontaneous preterm birth is stronger [1]. There are many potential pathways through which smoking may cause premature labor [2]. These include nicotine-induced vasoconstriction [3, 4], carbon monoxide-induced fetal hypoxia [5, 6], cadmium disruption of calcium signalling [7, 8], altered steroid hormone production [9, 10], changed responses to oxytocin [11, 12] and altered prostaglandin (PG) production and metabolism [13].

The use of animal models to investigate potential mechanisms from preterm birth has shifted from endocrine pathways (e.g. cortisol induced placental progesterone withdrawal in sheep; luteolysis in rats) to inflammatory models e.g. lipopolysaccharide (LPS) induced proinflammatory response in mice [14]. The induction of premature labor by LPS in mice has highlighted the importance of genes involved in the regulation of connective tissue remodelling and tensile strength such as tenascin

(*Tnc*) and thrombospondin (*Thhs2*) as well as the activity of several matrix metalloproteinases [15].

These advances have contributed to our understanding of cervical ripening and dilatation mechanisms associated with spontaneous preterm labor.

Amnion choriodecidual (ACD) cells, especially tissue macrophages, may have a role in spontaneous preterm labor by promoting the release of prostaglandins and proinflammatory cytokines [16].

Whilst the amnion produces large quantities of PGE₂, the chorion produces both PGE₂ and PGF₂ α as well as an important modulator of PG activity, 15-hydroxy PG dehydrogenase (HPGD) [17].

Proinflammatory cytokines (e.g. interleukin 1, tumour necrosis factor- α) promote upregulation of prostaglandin synthase enzymes in the fetal membranes and decidua [18]. Inflammation of the fetal membranes is much more common in preterm deliveries than at term: Acute chorioamnionitis has been detected in 30% of preterm pregnancies but only in 5% of term pregnancies [19, 20].

Chorioamnionitis causes early preterm labour by increasing prostaglandin production in ACD [21]; however the mechanism of labour in spontaneous preterm deliveries without signs of infection or inflammation remains unexplained. There is a complex interaction among maternal and fetal factors at the ACD interface; these involve prostaglandins, cytokines, growth factors and reactive oxygen species. These pathways are superimposed on genetic predisposition and immune defence mechanisms involved in the regulation of human labour [22]. The breakdown of maternal-fetal tolerance at the decidua/fetal membrane interface can disrupt the production of chemokines and cytokines (IL-1 α , TNF α), as well as prostaglandins, reactive oxygen radicals and proteases. These products can initiate uterine contractions directly and/or provoke cervical changes and premature rupture of the membranes [23].

Whilst smoking has been shown to affect the levels of prostaglandins, such as PGF₂ α , PGE₂, prostaglandin D₂ and the prostacyclin metabolite 6-ketoprostaglandin F₁ α [13] in amniotic fluid, the effect of smoking on protein expression within the fetal membranes and decidua has not previously been considered.

Here we present proteomic data using gel-free separation methods that allow the identification and measurement of relative changes of thousands of proteins simultaneously. The results show a very significant effect of smoking on the amnion/chorion/decidual proteome; enormous disruption caused by inflammatory infiltration and changes specifically associated with spontaneous term and preterm labor.

Materials and methods

Tissue collection

Fetal membrane tissue (combined amnion-chorion-decidua parietalis, ACD) was obtained immediately after delivery from women who were not in labor (NL; no uterine activity or cervical change) and were undergoing planned Caesarean section with the following indications: previous Caesarean section, previous obstetric anal sphincter injury or pelvic outlet obstruction. ACD samples were also obtained from women after vaginal deliveries following spontaneous labor (L). Cases were further divided into either term (TL or TNL; 37-42 weeks gestational age) or preterm (PTL; less than 35 weeks of gestation). PTL cases were further subdivided into those with evidence of inflammation/infection (PTLi) and those without (PTLn), based on clinical features of the women (pyrexia, offensive liquor or uterine tenderness) or histological determination of the presence of leucocyte infiltration in the fetal membranes (chorioamnionitis), decidua (deciduitis) or placenta (intervillositis), with or without maternal pyrexia or uterine tenderness. Smoking was determined by self-report. Tissues were snap-frozen in liquid nitrogen and stored at -80°C. This study was approved by the NHS South West Research Ethics Committee. All patients gave written informed consent.

Paraffin-embedded sections for histopathology

Tissues were rinsed in sterile saline and fixed in 4% phosphate buffered formaldehyde. After 24 hours fixation, tissues were washed with sterile saline and processed using Leica JUNG TP 1050 Tissue processor into paraffin wax and sectioned into 3 µm thickness.

1 Tissue homogenisation

2 Frozen tissue samples were homogenised in RIPA (Radio-ImmunoPrecipitation Assay) lysis buffer
3 (50mM Tris pH 7.5, 150mM sodium chloride, 1% NP-40, 0.1% SDS, 0.5% sodium deoxycholate, 1 x
4 Complete protease inhibitor cocktail (Roche), 1 x PhosSTOP protease inhibitor cocktail (Roche)) at
5 ~200 mg/ml using a Polytron homogeniser at room temperature. Homogenates were immediately
6 cleared by centrifugation at 16 000 g for 15 min at 4°C. Protein concentration was determined using
7 the Pierce™ BCA assay kit (ThermoFisher Scientific, Loughborough, UK). The supernatants were
8 adjusted by addition of further RIPA buffer to make each sample 175 µl at 2 mg/ml.

9 Tandem Mass Tag (TMT) Labelling and cation exchange chromatography

10 Aliquots of 100 µg of six samples per experiment were digested with trypsin (2.5 µg trypsin per 100
11 µg protein; 37°C, overnight), labelled with Tandem Mass Tag (TMT) sixplex reagents according to the
12 manufacturer's protocol (Thermo Fisher Scientific, Loughborough, UK) and the labelled samples
13 pooled.

14 A 50 µg aliquot of the pooled sample was used, evaporated to dryness and re-suspended in Buffer A
15 (10 mM KH₂PO₄, 25% MeCN, pH3) prior to fractionation by strong cation exchange using an Ettan LC
16 system (GE Healthcare). In brief, the sample was loaded onto a PolysulphoethylA column (100 x 2.1
17 mm, 5 µm, 200 Å; PolyLC Inc.) in buffer A and peptides eluted with an increasing gradient of buffer B
18 (10 mM KH₂PO₄, 25% MeCN, 1 M KCl, pH3) from 0 to 100% over 30 minutes. The resulting fractions
19 were evaporated to dryness, re-suspended in 5% (v/v) formic acid and then desalted using SepPak
20 cartridges according to the manufacturer's instructions (Waters, Milford, Massachusetts, USA).

21 Eluate from the SepPak cartridge was again evaporated to dryness and re-suspended in 1% formic
22 acid prior to analysis by nano-LC MSMS using an Orbitrap Fusion Tribrid Mass Spectrometer.

23 Nano-liquid chromatography mass spectrometry (Nano-LC MS)

24 The cation exchange fractions were further fractionated using an Ultimate 3000 nanoHPLC system in
25 line with an Orbitrap Fusion Tribrid mass spectrometer (Thermo Scientific). In brief, peptides in 1%

(v/v) formic acid were injected onto an Acclaim PepMap C18 nano-trap column (Thermo Scientific). After washing with 0.5% (v/v) acetonitrile 0.1% (v/v) formic acid, peptides were resolved on a 250 mm × 75 µm Acclaim PepMap C18 reverse phase analytical column (Thermo Scientific) over a 150 minute organic gradient, using 7 gradient segments (1-6% solvent B over 1 minute, 6-15% B over 58 minutes, 15-32% B over 58 minutes, 32-40% B over 5 minutes, 40-90% B over 1 minute, held at 90% B for 6 minutes and then reduced to 1% B over 1 minute) with a flow rate of 300 nl/minute. Solvent A was 0.1% formic acid and Solvent B was aqueous 80% acetonitrile in 0.1% formic acid. Peptides were ionised by nano-electrospray ionisation at 2 kV using a stainless-steel emitter with an internal diameter of 30 µm (Thermo Scientific) and a capillary temperature of 275°C.

All spectra were acquired using an Orbitrap Fusion Tribrid mass spectrometer controlled by Xcalibur 2.0 software (Thermo Scientific) and operated in data-dependent acquisition mode using an SPS-MS3 workflow. FTMS1 spectra were collected at a resolution of 120 000, with an automatic gain control (AGC) target of 400 000 and a maximum injection time of 100 ms. The top ten most intense ions were selected for MS/MS. Precursors were filtered according to charge state (to include charge states 2-6) and with monoisotopic precursor selection. Previously interrogated precursors were excluded using a dynamic window (40s +/-10ppm). The MS2 precursors were isolated with a quadrupole mass filter set to a width of 1.2m/z. ITMS2 spectra were collected with an AGC target of 5000, max injection time of 70 ms and CID collision energy of 35%.

For FTMS3 analysis, the Orbitrap was operated at 30 000 resolution with an AGC target of 50 000 and a max injection time of 105 ms. Precursors were fragmented by high energy collision dissociation (HCD) at a normalised collision energy of 55% to ensure maximal TMT reporter ion yield. Synchronous Precursor Selection (SPS) was enabled to include up to 10 MS2 fragment ions in the FTMS3 scan. The method allowed us to analyse the full proteome for each sample of ACD.

Data Analysis

The raw data files were processed and quantified using Proteome Discoverer software v1.4 (Thermo Scientific) and searched against the UniProt Human database (downloaded 08/11/14: 126385 entries) using the SEQUEST algorithm. Peptide precursor mass tolerance was set at 10 ppm, and MS/MS tolerance was set at 0.6 Da. Search criteria included oxidation of methionine (+15.9949) as a variable modification and carbamidomethylation of cysteine (+57.0214) and the addition of the TMT 6Plex mass tag (+229.163) to peptide N-termini and lysine as fixed modifications. Searches were performed with full tryptic digestion and a maximum of one missed cleavage was allowed. The reverse database search option was enabled and all peptide data was filtered to satisfy false discovery rate (FDR) of 5%.

Uniprot Human Database (<http://www.uniprot.org/uploadlists/>) was used to convert the accession numbers produced by the Proteome Discoverer software into Human Genome Organisation (HUGO) gene names. Where the accession numbers were not recognised by UniProt, the 'description' field output from Proteome Discoverer was analysed to find the 'GN' code where given and the HUGO gene name identified in this way.

Statistics

Median values are given unless otherwise stated and groups compared using the Kruskal-Wallis H test. Differences were deemed statistically significant for p values less than 0.05.

Results

ACD samples were collected from 20 women. The clinical characteristics for the placentas studied can be seen in table 1.

Table 1 Clinical characteristics for the 20 women giving ACD samples

Group	n	Median gestational age at delivery in weeks (range)	M:F	Median birthweight in kg (IQR)	Median length of labor in hours (IQR)	Median delivery to processing interval in mins (IQR)
All	20	36 ⁺³	8:12	2.61	3.2	114

		(24 ⁺¹ - 40 ⁺⁰)		(1.75 - 3.43)	(2.5 - 5.6)	(73 - 359)
Term, no labor (TNL)	5	39 ⁺¹ (39 ⁺⁰ - 39 ⁺⁴)	1:4	3.22 (3.00 - 3.39)	n/a	44 (33 - 60)
Term, labor (TL)	5	39 ⁺⁵ (38 ⁺⁰ - 40 ⁺⁰)	3:2	3.45 (3.43 - 3.53)	3.6 (2.8 - 6.9)	112 (98 - 165)
Preterm labor, no infection (PTLu)	4	33 ⁺¹ (31 ⁺⁵ - 34 ⁺⁴)	2:2	1.86 (1.75 - 2.02)	2.2 (1.1 - 3.7)	136 (49 - 388)
Preterm labor, infection (PTLi)	6	27 ⁺⁴ (24 ⁺¹ - 34 ⁺⁶)	2:4	1.01 (0.73 - 2.27)	5.8 (3.1 - 7.9)	97 (36 - 565)
Smoker	7	34 ⁺⁴ (24 ⁺¹ - 39 ⁺⁵)	3:4	1.90 (0.94 - 3.15)	4.4 (1.4 - 8.9)	44 (36 - 503)
Non-smoker	13	38 ⁺⁰ (26 ⁺⁰ - 40 ⁺⁰)	5:8	3.22 (1.94 - 3.46)	3.6 (2.7 - 4.6)	84 (49 - 171)

A combined total of 4709 proteins were detected within the 20 ACD samples. There were 243 proteins whose median level varied significantly among the different delivery groups (Kruskal-Wallis test; $p < 0.05$). Post-hoc analysis revealed between which of these groups the differences occurred. The magnitude of these changes (and their associated p values) are presented in tables 2-4. There were many more proteins with significant differences when comparing samples with inflammation (PTLi) with other groups; there were 105 proteins with altered expression between TNL and PTLi, but only 6 when comparing TNL with PTLn.

Proteins involved in prostaglandin synthesis, transport and degradation were detected. These included the transporter SLCO2A1, two enzymes involved in prostaglandin degradation HPGD and CBR1 (carbonyl reductase 1), and the prostaglandin synthases PTGES, PTGES2, PTGES3, and PTGDS. PTGS2 was not detected in any of the samples. None of these proteins altered significantly when comparing the delivery groups, except the enzyme 15-hydroxyprostaglandin dehydrogenase (HPGD). This enzyme was detected in all 20 samples and the median level was significantly reduced in the smokers relative to the non-smokers (0.43 fold, $p = 0.016$).

1 The differences in protein expression between the smokers and non-smokers, and between those
2 with and without evidence of inflammation can be seen in figure 1 and figure 2, respectively. In
3 these volcano plots each point represents a protein detected by proteomic analysis.
4 Myeloperoxidase (MPO), a peroxidase enzyme abundantly expressed in neutrophil granulocytes and
5 associated with inflammation, can be seen in the top right of the volcano plot in figure 1 showing
6 that MPO is significantly higher in the ACD samples from women with infectious/inflammatory
7 processes. HPGD can be seen in the top left of the volcano plot comparing the smokers and non-
8 smokers (figure 2), showing that the level of HPGD in the smokers is significantly reduced.

9

1 **Table 2 Protein changes associated with spontaneous labor at term**

Accession number	Gene symbol	Description	Ratio TNL:TL	p value
B7Z4R8	PRG4	Proteoglycan-4	3.36	0.016
P0COL5	C4B	Complement C4-B	1.91	0.042
A8K5J8	C1R	Complement C1R subcomponent	1.58	0.037
P62306	SNRPF	Small nuclear ribonucleoprotein F	1.28	0.017
B4DKI2	SORB	cDNA FLJ60282, highly similar to Sorbitol dehydrogenase	1.20	0.038
B4E2S3	RFTN1	Raftlin	0.77	0.043
P49411	TUFM	Elongation factor Tu, mitochondrial	0.76	0.023
P54577	YARS	Tyrosine--tRNA ligase, cytoplasmic	0.72	0.038
P62070	RRAS2	Ras-related protein R-Ras2	0.66	0.038
K7ENK9	VAMP2	Vesicle-associated membrane protein 2	0.64	0.028
F8W8T1	MX1	Interferon-induced GTP-binding protein Mx1	0.58	0.017
Q14166	TTL12	Tubulin--tyrosine ligase-like protein 12	0.57	0.045
P05161	ISG15	Ubiquitin-like protein ISG15	0.45	0.041
P00966	ASS1	Argininosuccinate synthase	0.31	0.045

2

1 **Table 3 Proteins altered by the presence of inflammation.** For brevity, only proteins with at least a 2-fold
2 difference are shown.

Accession number	Gene symbol	Description	Ratio TNL:PTLi	p value
P17213	BPI	Bactericidal permeability-increasing protein	21.46	0.007
C9JZR7	ACTB	Actin, cytoplasmic 1	18.66	0.016
B2MUD5	ELA2	Neutrophil elastase	15.54	0.003
B2R4M6	S100	Protein S100	15.43	0.002
P59666	DEFA3	Neutrophil defensin 3	10.53	0.029
P05164	MPO	Myeloperoxidase	10.22	0.008
P27216	ANXA13	Annexin A13	10.13	0.024
P80188	LCN2	Neutrophil gelatinase-associated lipocalin	10.13	0.002
Q96IS6	HSPA8	HSPA8 protein	8.73	0.003
P08311	CTSG	Cathepsin G	8.58	0.006
P05109	S100A8	Protein S100-A8	7.67	0.014
P54108	CRISP3	Cysteine-rich secretory protein 3	7.01	0.016
Q9NS13	APOB48R	Placenta apolipoprotein B48 receptor type 2	6.42	0.009
B3KTE6	CHI3L1	Chitinase-3-like protein 1	6.34	0.034
P49913	CAMP	Cathelicidin antimicrobial peptide	5.99	0.003
E7EQB2	LTF	Lactotransferrin	5.45	0.021
Q6P4A8	PLBD1	Phospholipase B-like 1	5.17	0.023
H7C2Z6	GCA	Grancalcin	4.91	0.016
P52790	HK3	Hexokinase-3	4.73	0.038
P43490	NAMPT	Nicotinamide phosphoribosyltransferase	4.29	0.002
P14317	HCLS1	Hematopoietic lineage cell-specific protein	3.87	0.032
A0A024R936	NCF2	Neutrophil cytosolic factor 2 (65kDa, chronic granulomatous disease, autosomal 2), isoform CRA_a	3.73	0.012
E9PAQ1	CFP	Properdin	3.44	0.034
P31146	CORO1A	Coronin-1A	3.43	0.014
O00160	MYO1F	Unconventional myosin-I _f	3.02	0.023
P16401	HIST1H1B	Histone H1.5	2.98	0.003
P12429	ANXA3	Annexin A3	2.97	0.015
X6R433	PTPRC	Receptor-type tyrosine-protein phosphatase C	2.93	0.027
Q10588	BST1	ADP-ribosyl cyclase/cyclic ADP-ribose hydrolase 2	2.68	0.041
P20700	LMNB1	Lamin-B1	2.53	0.01
B3KSI4	TKT	Transketolase	2.41	0.012
A0A024RAJ8	IQGAP2	IQ motif containing GTPase activating protein 2, isoform CRA_b	2.32	0.012
C9JQ42	GYG1	Glycogenin-1	2.24	0.021
Q08722	CD47	Leukocyte surface antigen CD47	2.19	0.013
B5BU83	STMN1	Stathmin	2.15	0.011
P13796	LCP1	Plastin-2	2.12	0.049

P16402	HIST1H1D	Histone H1.3	2.06	0.028
P08133	ANXA6	Annexin A6	2.01	0.022
A6XND0	IGFBP3	Insulin-like growth factor binding protein 3	0.50	0.013
Q8IV56	PRR15	Proline-rich protein 15	0.50	0.04
E4W6B6	RPL27	RPL27/NME2 fusion protein	0.49	0.036
J3QSB5	RPL36	60S ribosomal protein L36	0.49	0.009
P04181	OAT	Ornithine aminotransferase, mitochondrial	0.46	0.025
P35237	SERPINB6	Serpin B6	0.44	0.027
C9J7T7	NCOR2	Nuclear receptor corepressor 2	0.43	0.03
O94907	DKK1	Dickkopf-related protein 1	0.41	0.013
B4DP54	TUBB6	Tubulin beta-6 chain	0.41	0.007
P50479	PDLIM4	PDZ and LIM domain protein 4	0.23	0.013

1

2

1 **Table 4 Proteins altered by maternal smoking.** For brevity, only proteins with at least a 2-fold difference are
2 shown.

3

Accession number	Gene symbol	Description	Ratio Smokers:non-smokers	p value
A2NX48	BPI'	Bactericidal /Permeability Increasing Protein	8.69	0.005
Q6P4A8	PLBD1	Phospholipase B-like 1	3.63	0.024
P27105	STOM	Erythrocyte band 7 integral membrane protein	2.61	0.017
P17948	FLT1	Vascular endothelial growth factor receptor 1	0.48	0.003
Q6P988	NOTUM	Protein notum homolog	0.47	0.005
H0YK49	ETFA	Electron transfer flavoprotein subunit alpha, mitochondrial	0.47	0.037
J3QRL9	DSC3	Desmocollin-3	0.45	0.037
P15428	HPGD	15-hydroxyprostaglandin dehydrogenase	0.43	0.016
E7EPP8	CYP11A1	Cholesterol side-chain cleavage enzyme, mitochondrial	0.40	0.030
I3L3H2	EIF4A3	Eukaryotic initiation factor 4A-III	0.39	0.037
A0A024R6I7	SERPINA1	Alpha-1-antitrypsin	0.24	0.003

Figure 1 Volcano plot to show difference in protein expression between ACD samples with evidence of inflammation/infection and those without. The X axis represents the fold difference, with those furthest from the midline the point showing greatest differences between the two groups. The axis is logarithmically converted so that \log_2 (fold difference) is plotted. Therefore a plotted value of greater than 1 or less than -1 indicates a fold difference of more than 2. \log_2 (fold difference) > 2.5 correlates to fold difference >5.7. The Y axis represents the p value. It is shown as $-\log_{10}$ (p value) and therefore the higher the point the more statistically significant the difference between the two groups. $-\log_{10}$ (p value) >1.3 correlates to p value <0.05. Proteins with larger fold differences that had p values <0.05 ($-\log_{10}$ (p value) >1.3) are labelled with their gene names and marked with rhomboids.

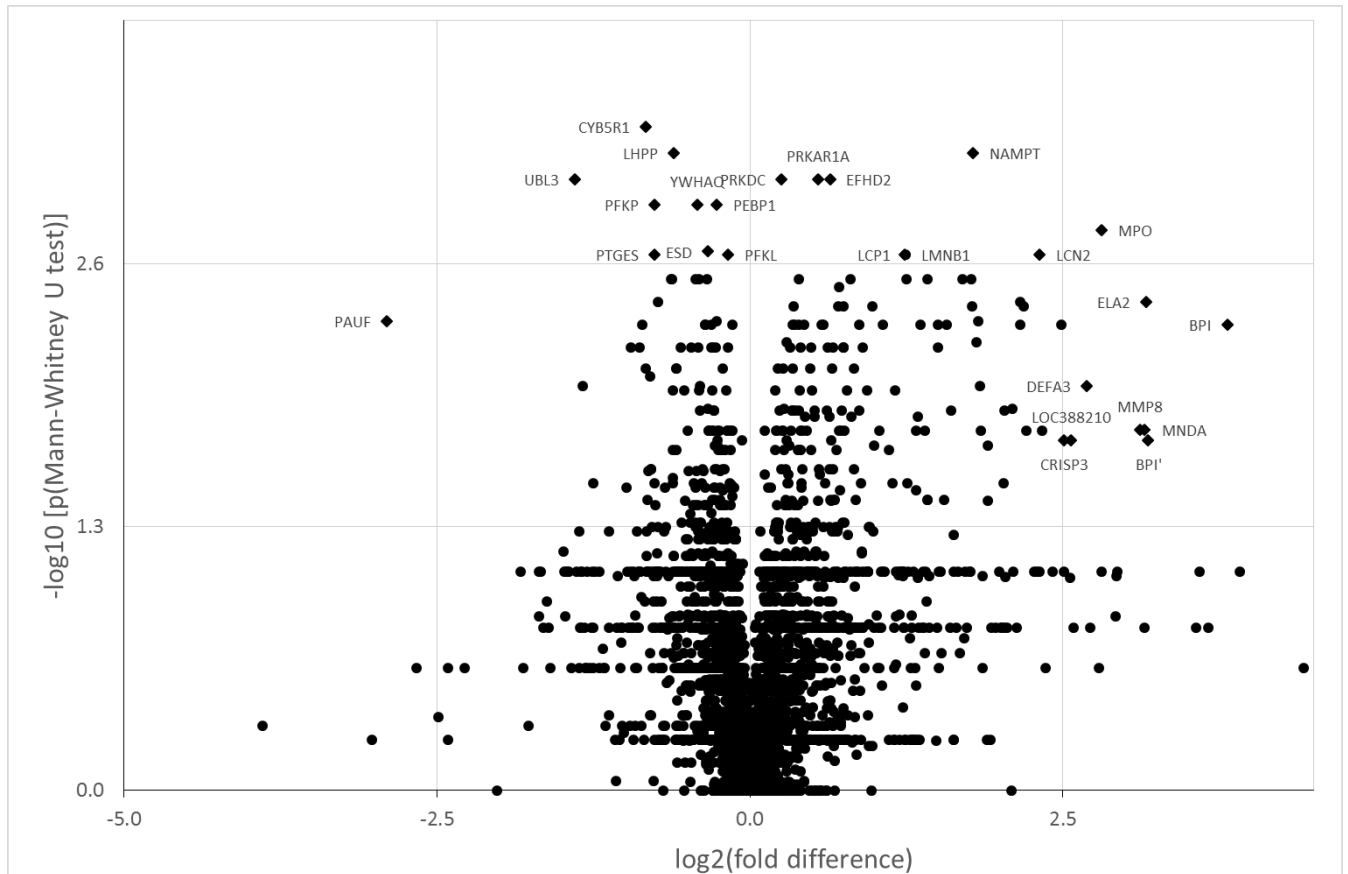
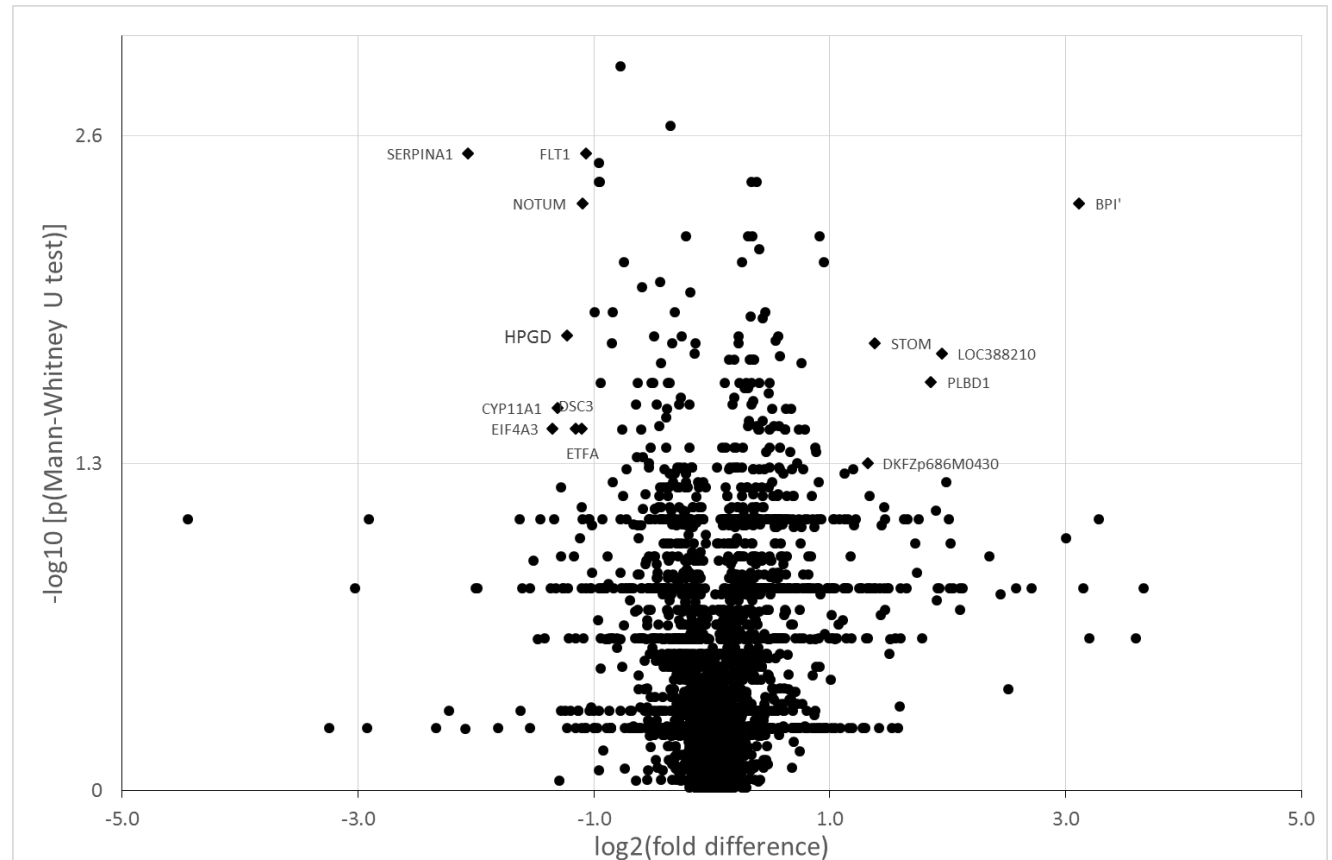


Figure 2 Volcano plot to show difference in protein expression between those ACD samples from smokers and non-smokers. The X axis represents the fold difference, with those furthest from the midline point showing greatest differences between the two groups. The axis is logarithmically converted so that \log_2 (fold difference) is plotted. Therefore a plotted value of greater than 1 or less than -1 indicates a fold difference of more than 2. The Y axis represents the p value. It is shown as $-\log_{10}$ (p value) and therefore the higher the point the more statistically significant the difference between the two groups. $-\log_{10}$ (p value) >1.3 correlates to p value <0.05. Proteins with larger fold differences that had p values <0.05 are labelled with their gene names and marked as rhomboids.



Discussion

The fetal membranes and decidua have important tasks, not only containing the developing fetus and amniotic fluid, and providing an essential physical barrier, but also in being the main interface between mother and baby, ideally situated to receive both maternal and fetal signals as well as transmit signals to the myometrium [17]. Here we report the investigation of their vital paracrine functions using tandem mass tagging liquid chromatography mass spectrometry (TMT-LC MS) for the first time. TMT-LC MS gives quantitative information on the abundance of proteins and doesn't rely on the availability of suitable antibodies, a considerable limitation of immunoblotting techniques.

Effects of labor and inflammation

1 Increased levels of the PG synthases within the labor and inflammation groups were anticipated. The
2 prostaglandin F synthase AKR1B1 (aldo-keto reductase family 1 member B) was detected in all 20
3 samples; no differences in this enzyme were discernible when comparing the samples from the labor
4 and non-labor groups. One explanation for this surprising result is that the decidual component of
5 the ACD samples is impacting on the AKR1B1 levels [25]. Harper et al. in 1983 described higher
6 decidual levels of PGF2 α in pre-labor samples when compared with labor samples [26], so it is
7 possible that this PGF2 α is a consequence of a labor-associated decrease in decidual AKR1B1, which
8 would balance out any potential increases in the amnion/chorion. Complement-related proteins are
9 often identified in maternal plasma [27] and are synthesised by ACD tissues [28] but their predictive
10 value in the timing of the onset of spontaneous labor is poor [29]. We found a modest decrease in
11 C1R (Complement C1r subcomponent) with labor at term; C1R is involved in the classical pathway of
12 complement activation. RFTN1 (raftlin) is a lipid raft protein involved in T cell receptor signalling [30]
13 and our findings suggest it may increase in association with immune activation in labor.

14 Inflammation caused significant disruption in nearly 50 proteins in ACD which is a reflection of the
15 activation of resident ACD macrophages and infiltrating leukocytes previously studied at the
16 transcriptomic level [31, 32]. The observed increase in MPO (myeloperoxidase; part of the leukocyte
17 defense system) with inflammatory changes is reassuring; MPO levels in amniotic fluid have been
18 shown to increase in chorioamnionitis, most likely representing high levels of neutrophil activation
19 and degranulation [33, 34]. Labor did not affect MPO expression. The effect of labor on MPO
20 expression in ACD has not previously been investigated. Many authors have suggested a degree of
21 inflammatory activity is associated with normal labor [35-37]; Haddad et al. found that labor
22 produced gene expression changes in keeping with localised inflammation [38], even when
23 histologically detectable inflammation was absent. Whilst spontaneous labor has been associated
24 with elevated levels of chemokines known to be involved in monocyte recruitment [38], neutrophil
25 infiltration and activation leading to MPO production are not thought to be a significant component

of the initiation of labor. Myometrial inflammation is likely to be a consequence rather than a cause of labor [39].

Effects of smoking

Smoking has previously been shown to increase fetal membrane and amniotic fluid levels of $\text{PGF2}\alpha$, PGE2 , PGD2 and the prostaglandin-like F2-isoprostane , a marker for oxidative stress [13, 40]. In our study, maternal smoking significantly affected expression of the key enzyme involved in the inactivation of prostaglandins, 15-hydroxy prostaglandin dehydrogenase (HPGD) [41]; ACD samples from smokers had less than half the level of HPGD than those from the non-smokers (figure 2).

Genetically modified mice with decreased expression of HPGD deliver prematurely without progesterone-withdrawal [42]. In these animals the onset of labor was preceded by increased concentrations of PGE2 and $\text{PGF2}\alpha$. The exact role of HPGD in initiating labor is unclear. Whilst several authors have described lower levels of HPGD expression in the fetal membranes in association with labor [32, 43, 44], others have reported no labor-associated change in the expression and activity of the enzyme [45] or an increase in labor-associated activity [46]. Some authors have proposed that there is an altered expression of HPGD in preterm labor, with 15-20% of patients in idiopathic preterm labor exhibiting decreased HPGD protein in the chorion as well as reduced HPGD activity [43]. With infection-associated PTL both no change [43] and reduced activity and expression of HPGD have been reported [32, 45]. Johnson et al. suggest that the variation in these findings is due to the in vitro nature of much of this work [41]; HPGD protein turnover is rapid and altered by some of the agonists used in cell culture. Using primers that recognise all splice variants they showed that the total abundance of HPGD mRNA did not change with labor. There was no effect of labor, inflammatory status or gestational age on the HPGD levels in our ACD samples.

The effect of maternal smoking on HPGD expression is a novel interesting finding. We are unaware of any studies that have examined the effect of tobacco smoke on HPGD expression. Furthermore, those studies that looked at the effect of gestational age, labor and inflammatory status on HPGD

expression [32, 43-45] did not appear to have considered maternal smoking as a co-factor. We propose that the reduced expression of HPGD associated with smoking is a novel mechanism through which smoking may contribute to preterm labor. Lower levels of this enzyme, key to metabolising prostaglandins, may result in higher levels of prostaglandins and therefore precipitate labor prematurely.

Limitations

The limitations of using self-reported smoking behaviour to define smokers are well documented [47-49] and objective measures of smoking exposure may be preferable. Exhaled carbon monoxide (eCO) readings have been shown to be reliable in differentiating smokers from non-smokers [50-52]. Whilst some women had first trimester eCO readings available, more than half did not. Smoking status was therefore defined by self-report despite its limitations. Furthermore, the importance of environmental tobacco smoke exposure on pregnancy outcomes is increasingly being recognised [53] as well as an individual's past smoking habits. Future work on the effect of smoking on gestational tissues' protein expression should give consideration to the use of biochemical measures to define smoking exposure, both direct and passive. Serum or hair cotinine or nicotine levels have the ability to give exposure information on greater timeframes than eCO [49].

Chorioamnionitis, as determined by histopathological examination of the placental tissues, is clinically silent in the majority of women [54]. In our data, half of the samples subsequently found to have histopathological features suggestive of acute infection (presence of leucocyte infiltration in the fetal membranes, decidua or placenta) came from women with no clinical signs or symptoms of chorioamnionitis. Placental swab culture, including bacterial PCR testing could be used in conjunction with measuring the expression of other proteins known to be involved in inflammatory responses such as interleukin 8, S100 calcium binding protein A8 and Toll-like receptor 2 [32] to further facilitate classification of the samples. Whilst median levels of MPO were found to be raised

1 in the inflammatory group, values were too varied to use this measure to further categorise the
2 samples.

3 This paper confirms the potential of TMT proteomics to identify multiple protein changes in ACD in
4 relation to labor, inflammation and smoking. It is important to use reliable validated databases and
5 an accepted, stringent false discovery rates (FDR) estimation. Here we have used a recommended
6 FDR of 5% [55]. However, even assuming reliable identification and quantification of a protein, the
7 data doesn't inform us of its biological activity. There are considerable splice variants and post-
8 translational modifications that alter the functionality of a protein; many proteins have multiple
9 functions or may exist as active and inactive isoforms [55]. In some cases proteins known to be
10 present in the samples may not be detected by TMT-LC MS. This may either be because there are
11 insufficient amounts in the sample, because a given peptide's signal is masked by another peptide's
12 signal within the mass spectrometer, or because a certain protein does not produce tryptic peptides
13 of a suitable size.

14 Despite these limitations proteomics is a powerful tool for the discovery of new proteins of interest.
15 Our finding of lower HPGD levels in the ACD samples from smokers raises important questions
16 regarding the effect of smoking on the mechanism of preterm labor. Further research is required,
17 including the use of functional assays to demonstrate any effect of smoking on the activity of HPGD,
18 and the range of prostaglandin metabolites produced.

Acknowledgements

This work was supported by the British Maternal and Fetal Medicine Society and Action Medical Research [grant number SP4612].

References

1. Kyrklund-Blomberg, N.B. and S. Cnattingius, *Preterm birth and maternal smoking: risks related to gestational age and onset of delivery*. Am J Obstet Gynecol, 1998. **179**(4): p. 1051-5.
2. Ion, R. and A.L. Bernal, *Smoking and Preterm Birth*. Reprod Sci, 2015. **22**(8): p. 918-26.
3. Goldstein, H., et al., *Cigarette smoking and prematurity*. Public Health Rep, 1964. **79**: p. 553-60.
4. Suzuki, K., L.J. Minei, and E.E. Johnson, *Effect of nicotine upon uterine blood flow in the pregnant rhesus monkey*. Am J Obstet Gynecol, 1980. **136**(8): p. 1009-13.
5. Longo, L.D., *The biological effects of carbon monoxide on the pregnant woman, fetus, and newborn infant*. Am J Obstet Gynecol, 1977. **129**(1): p. 69-103.
6. Liu, S., et al., *Association between gaseous ambient air pollutants and adverse pregnancy outcomes in Vancouver, Canada*. Environ Health Perspect, 2003. **111**(14): p. 1773-8.
7. Nishijo, M., et al., *Effects of maternal exposure to cadmium on pregnancy outcome and breast milk*. Occup Environ Med, 2002. **59**(6): p. 394-6; discussion 397.
8. Sipowicz, M., et al., *Effects of cadmium on myometrial activity of the nonpregnant human. Interactions with calcium and oxytocin*. Acta Obstet Gynecol Scand, 1995. **74**(2): p. 93-6.
9. Piasek, M. and J.W. Laskey, *Acute cadmium exposure and ovarian steroidogenesis in cycling and pregnant rats*. Reprod Toxicol, 1994. **8**(6): p. 495-507.
10. Ng, S.P., et al., *Hormonal changes accompanying cigarette smoke-induced preterm births in a mouse model*. Exp Biol Med (Maywood), 2006. **231**(8): p. 1403-9.
11. Egawa, M., et al., *Smoking enhances oxytocin-induced rhythmic myometrial contraction*. Biol Reprod, 2003. **68**(6): p. 2274-80.
12. Kanamori, C., et al., *Effect of cigarette smoking on mRNA and protein levels of oxytocin receptor and on contractile sensitivity of uterine myometrium to oxytocin in pregnant women*. Eur J Obstet Gynecol Reprod Biol, 2014. **178**: p. 142-7.
13. Menon, R., et al., *Amniotic fluid eicosanoids in preterm and term births: effects of risk factors for spontaneous preterm labor*. Obstet Gynecol, 2011. **118**(1): p. 121-34.
14. Nielsen, B.W., et al., *A Cross-Species Analysis of Animal Models for the Investigation of Preterm Birth Mechanisms*. Reprod Sci, 2016. **23**(4): p. 482-91.
15. Mahendroo, M., *Cervical remodeling in term and preterm birth: insights from an animal model*. Reproduction, 2012. **143**(4): p. 429-38.
16. Nagamatsu, T. and D.J. Schust, *The immunomodulatory roles of macrophages at the maternal-fetal interface*. Reprod Sci, 2010. **17**(3): p. 209-18.
17. Myatt, L. and K. Sun, *Role of fetal membranes in signaling of fetal maturation and parturition*. Int J Dev Biol, 2010. **54**.
18. Norwitz, E.R., A. Lopez Bernal, and P.M. Starkey, *Tumor necrosis factor-alpha selectively stimulates prostaglandin F2 alpha production by macrophages in human term decidua*. Am J Obstet Gynecol, 1992. **167**(3): p. 815-20.
19. Hillier, S.L., et al., *A case-control study of chorioamnionic infection and histologic chorioamnionitis in prematurity*. N Engl J Med, 1988. **319**(15): p. 972-8.
20. Horvath, B., et al., *Silent chorioamnionitis and associated pregnancy outcomes: a review of clinical data gathered over a 16-year period*. J Perinat Med, 2014. **42**(4): p. 441-7.
21. López Bernal, A., et al., *Prostaglandin E production by the fetal membranes in unexplained preterm labour and preterm labour associated with chorioamnionitis*. Br J Obstet Gynaecol, 1989. **96**.

22. Norwitz, E.R., et al., *Molecular Regulation of Parturition: The Role of the Decidual Clock*. Cold Spring Harb Perspect Med, 2015. **5**(11).
23. Romero, R., S.K. Dey, and S.J. Fisher, *Preterm labor: one syndrome, many causes*. Science, 2014. **345**(6198): p. 760-5.
24. Nelson, D.M. and G.J. Burton, *A technical note to improve the reporting of studies of the human placenta*. Placenta, 2011. **32**(2): p. 195-6.
25. Alzamil, H.A., et al., *Expression of the prostaglandin F synthase AKR1B1 and the prostaglandin transporter SLCO2A1 in human fetal membranes in relation to spontaneous term and preterm labor*. Front Physiol, 2014. **5**: p. 272.
26. Harper, M.J., G.S. Khodr, and G. Valenzuela, *Prostaglandin production by human term placentas in vitro*. Prostaglandins Leukot Med, 1983. **11**(1): p. 121-9.
27. Scholl, P.F., et al., *Maternal serum proteome changes between the first and third trimester of pregnancy in rural southern Nepal*. Placenta, 2012. **33**(5): p. 424-32.
28. Goldberg, M., et al., *Synthesis of complement proteins in the human chorion is differentially regulated by cytokines*. Mol Immunol, 2007. **44**(7): p. 1737-42.
29. Kovar, I.Z. and P.G. Riches, *C3 and C4 complement components and acute phase proteins in late pregnancy and parturition*. J Clin Pathol, 1988. **41**(6): p. 650-2.
30. Saeki, K., et al., *A major lipid raft protein raftlin modulates T cell receptor signaling and enhances th17-mediated autoimmune responses*. J Immunol, 2009. **182**(10): p. 5929-37.
31. Rinaldi, S.F., et al., *Immune cell and transcriptomic analysis of the human decidua in term and preterm parturition*. Mol Hum Reprod, 2017. **23**(10): p. 708-724.
32. Phillips, R.J., M.A. Fortier, and A. Lopez Bernal, *Prostaglandin pathway gene expression in human placenta, amnion and choriodecidua is differentially affected by preterm and term labour and by uterine inflammation*. BMC Pregnancy Childbirth, 2014. **14**: p. 241.
33. Tambor, V., et al., *Proteomics and bioinformatics analysis reveal underlying pathways of infection associated histologic chorioamnionitis in pPROM*. Placenta. **34**(2): p. 155-161.
34. Wolfe, K.B., et al., *Modulation of lipopolysaccharide-induced chorioamnionitis in fetal sheep by maternal betamethasone*. Reprod Sci, 2013. **20**(12): p. 1447-54.
35. Hillier, S.L., et al., *The relationship of amniotic fluid cytokines and preterm delivery, amniotic fluid infection, histologic chorioamnionitis, and chorioamnion infection*. Obstet Gynecol, 1993. **81**.
36. Steinborn, A., et al., *Elevated placental cytokine release, a process associated with preterm labor in the absence of intrauterine infection*. Obstet Gynecol, 1996. **88**.
37. Keelan, J.A., et al., *Cytokines, Prostaglandins and Parturition—A Review*. Placenta, 2003. **24**: p. S33-S46.
38. Haddad, R., et al., *Human spontaneous labor without histologic chorioamnionitis is characterized by an acute inflammation gene expression signature*. American Journal of Obstetrics and Gynecology, 2006. **195**(2): p. 394-405.e12.
39. Singh, N., et al., *Is myometrial inflammation a cause or a consequence of term human labour?* J Endocrinol, 2017. **235**(1): p. 69-83.
40. Menon, R., et al., *Cigarette smoke induces oxidative stress and apoptosis in normal term fetal membranes*. Placenta, 2011. **32**(4): p. 317-22.
41. Johnson, R.F., et al., *Regulation of 15-hydroxyprostaglandin dehydrogenase (PGDH) gene activity, messenger ribonucleic acid processing, and protein abundance in the human chorion in late gestation and labor*. J Clin Endocrinol Metab, 2004. **89**(11): p. 5639-48.
42. Roizen, J.D., et al., *Preterm birth without progesterone withdrawal in 15-hydroxyprostaglandin dehydrogenase hypomorphic mice*. Mol Endocrinol, 2008. **22**.
43. Sangha, R.K., et al., *Immunohistochemical localization, messenger ribonucleic acid abundance, and activity of 15-hydroxyprostaglandin dehydrogenase in placenta and fetal membranes during term and preterm labor*. J Clin Endocrinol Metabol, 1994. **78**.

44. Pomini, F., et al., *Activity and expression of 15-hydroxyprostaglandin dehydrogenase in cultured chorionic trophoblast and villous trophoblast cells and in chorionic explants at term with and without spontaneous labor*. Am J Obstet Gynecol, 2000. **182**.
45. van Meir, C.A., et al., *15-hydroxyprostaglandin dehydrogenase: implications in preterm labor with and without ascending infection*. J Clin Endocrinal Metab, 1997. **82**.
46. Mitchell, B.F., K. Rogers, and S. Wong, *The dynamics of prostaglandin metabolism in human fetal membranes and decidua around the time of parturition*. J Clin Endocrinol Metab, 1993. **77**(3): p. 759-64.
47. Shipton, D., et al., *Reliability of self reported smoking status by pregnant women for estimating smoking prevalence: a retrospective, cross sectional study*. BMJ, 2009. **339**: p. b4347.
48. Bardy, A.H., et al., *Objectively measured tobacco exposure during pregnancy: neonatal effects and relation to maternal smoking*. Br J Obstet Gynaecol, 1993. **100**(8): p. 721-6.
49. Eliopoulos, C., et al., *Hair concentrations of nicotine and cotinine in women and their newborn infants*. JAMA, 1994. **271**(8): p. 621-3.
50. Seidman, D.S., et al., *Noninvasive validation of tobacco smoke exposure in late pregnancy using end-tidal carbon monoxide measurements*. J Perinatol, 1999. **19**(5): p. 358-61.
51. Bailey, B.A., *Using expired air carbon monoxide to determine smoking status during pregnancy: preliminary identification of an appropriately sensitive and specific cut-point*. Addict Behav, 2013. **38**(10): p. 2547-50.
52. Campbell, E., R. Sanson-Fisher, and R. Walsh, *Smoking status in pregnant women assessment of self-report against carbon monoxide (CO)*. Addict Behav, 2001. **26**(1): p. 1-9.
53. Ion, R.C., A.K. Wills, and A.L. Bernal, *Environmental Tobacco Smoke Exposure in Pregnancy is Associated With Earlier Delivery and Reduced Birth Weight*. Reprod Sci, 2015. **22**(12): p. 1603-11.
54. Andrews, W.W., et al., *The Alabama Preterm Birth study: polymorphonuclear and mononuclear cell placental infiltrations, other markers of inflammation, and outcomes in 23- to 32-week preterm newborn infants*. Am J Obstet Gynecol, 2006. **195**(3): p. 803-8.
55. Rabilloud, T. and P. Lescuyer, *The proteomic to biology inference, a frequently overlooked concern in the interpretation of proteomic data: a plea for functional validation*. Proteomics, 2014. **14**(2-3): p. 157-61.